D. L. B. Jupp
K. K. Mayo
Division of Land Use Research
CSIRO
Canberra, A.C.T. 2601, Australia

The Use of Residual Images in Landsat Image Analysis

The method consists of developing two images from a classification: A mean image in which the pixels in the class are assigned the class mean, and a residual image in which the pixels are assigned the difference between the raw data and the mean.

Introduction

When classifications such as land use or land cover are produced from Landsat data, or produced independently and combined with Landsat data, there is a recurring problem of precision (i.e., whether the classification is sufficiently fine) in the classified image (or map). For example, cross spectral plots of Band 7 against Band 5 and their histograms for each class may show class heterogeneity in the form of distinct sub-classes. This heterogeneity would usually indicate the need for further subdivision into spectral sub-classes. However, this type of analysis does not show whether the effects arise from important (unmapped) spatial patterns and textures, or from transient physical effects which are unique to the Landsat image, and does not locate the heterogeneities for subsequent retraining of the classifier.

The need to distinguish between important land-cover classes and sub-classes accounting for spectral heterogeneity in the image reflects the distinction between 'structural' classes and Landsat 'data' classes. The structural model, in statistics, is the set of defining relations of the system being studied (Joreskog, 1973) and the data model is the set of measures on the system together with noise and errors of measurement. A data (or 'spectral') class is a set of individual picture elements (pixels) which is statistically homogeneous in terms of the measurements, and might be loosely described in Landsat images as a set of pixels with similar color. Typically, spectral classes might be generated by unsupervised clustering. The structural (or 'land-cover') classes, on the other hand, such as the forest, urban, open grassland, and other land-cover classes described later, are rarely spectrally homogeneous (Jupp *et al.*, 1979), and as a consequence need careful definition, or separation into spectral subclasses, if they are to be mapped from Landsat data (Haralick, 1976).

Abstract: *A method for interactively analyzing classified images and enhancing patterns with low contrast is introduced. It consists of generating one image in which each pixel is assigned the class mean radiance (the 'mean' image) and another in which each pixel is assigned the difference between the raw data and the class mean (the 'residual' image). It is shown how these two images expand the scope of the post-classification display and analysis and how residual images can be used to enhance subtle patterns in a Landsat image. Examples of application to land-cover and spectral classification are given, and the applicability of the method beyond Landsat data are discussed.*

An analysis of classification precision, which uses the capabilities of an interactive image display and analysis system, can be obtained by generating two new images from any classification of Landsat data. These are

- The 'mean' image, in which the radiance values for the four Landsat bands are replaced over the whole image by the means of the classes to which the pixels belong; and
- The 'residual' image, in which each pixel is given the difference between the class mean and the actual radiance values.

Photogrammetric Engineering and Remote Sensing,
Vol. 48, No. 4, April 1982, pp. 595-604.

0099-1112/82/4804-605$02.25/0

The two images can be analyzed by any of the standard methods of pattern enhancement and picture processing, such as Karhunen-Loeve (or principal component) transformation of the residual image, level slicing, ratioing, classification, and histogram equalization.

The Mean Image

Replacing the original image by a mean image and a residual image may be regarded as a form of data dependent, and non-stationary, low pass filtering. The residual image contains the high pass data. The mean image (which is equivalent to Abotteen's cluster image (Abotteen, 1979)), as a display of the classification, is a smoothed and cleaned (in that boundaries are sharpened) version of the original image.

The mean image is a color-coded classification map, but differs from the usual color-coded product of classifiers, in which it is often not easy to relate the colors of the classes back to the original scene, and in which the color coding may bear no relation to the spectral similarity between classes. The color coding of the mean image can be particularly useful when land-cover classes are being displayed, since the mean image can provide a visual estimate of class similarity. However, it is important to note that color similarity and statistical similarity are related in a complex fashion (Wyszecki and Stiles, 1967).

Murai (1975) recognized that the usual color coding to land-cover classes lost an appreciable amount of information. He associated the three primary colors with three 'primary' land covers (Vegetation (green), Water (blue), Non-organic matter (red)) and displayed classes as mixtures of these. The mean image does not attempt such a primary classification, but does result in a false color image which keys color and tone with class type and similarity.

There are some disadvantages with the mean image. The first is that, as with any color-coded classification, it does not display within-class variance, nor the existance of gradients. This is a good reason for always viewing the residual image. The second disadvantage is that similar classes can often be difficult to distinguish in the mean image. This second disadvantage can, however, be overcome by coding selected classes to distinct colors with the mean image as background.

The Residual Image

The question of how well the mean represents the spectral variation in the original image is best answered by an analysis of the residual image.

When the pixels have been coded to land-cover classes, such as land covers mapped from aerial photographs and ground survey, some of the variations in the residual image may arise from registration errors and real changes in the area between the time of the Landsat overpass and the land-cover mapping. (Using the residual image for change detection is not pursued in this paper.) Despite these differences, the most significant residuals will be spectral heterogeneities in the form of distinct spectral sub-classes within and across the land-cover class boundaries. The advantage of the analysis proposed here is that the extent to which these variations arise from unmapped land covers, which are identifiable as structural units, can often be assessed using interactive analysis of the residual image.

On the other hand, the classification of pixels to classes may have been accomplished by supervised or unsupervised classifiers. Here, the classes are spectral classes, and the residual image can indicate whether classes should be further subdivided into sub-classes or redefined to adequately map the spectral variations in the original image.

A familiar example of a trade-off between these situations occurs when land-cover classes need to be subdivided into spectral sub-classes to improve trained classifier performance (Haralick, 1976) as in Example 1 below. Here, the spectral heterogeneity of the land-cover class is being mollified by subdivision, and the residual image provides a means for locating training areas for the subclasses. For example, in the image studied in Example 1 below, the major variation within the Forest Class is due to radiance variations across topography. 'Bright' and 'shaded' spectral subclasses within Forest might therefore provide a means of improving forest recognition in trained classifiers. Subsequent residual images would be obtained by subtracting subclass means.

A separate, and possibly very significant, use of the residual image is to detect non-hierarchical classes and patterns. For example, soil boundaries and human activity cannot be easily accomodated in a hierarchical scheme, since they overlap spatially with settlement boundaries dominating the Landsat recorded radiance. If generalized classes are chosen which adequately map the settlement patterns, then the residual image can enhance patterns which cut across these major class boundaries by the local contrast reductions.

Residual and Standardized Residual Images

A reference model which can be used to measure departure in the residual image by statistical methods is the simple 'signature' model, in which each class is assumed to be characterized by a constant signature of radiance

$$\mathbf{r}_k = \begin{bmatrix} r_{1k} \\ r_{2k} \\ r_{3k} \\ r_{4k} \end{bmatrix} \text{(for class } k\text{)}$$

in the four Landsat bands. The observed radiances of pixels in class k are assumed to show spatially stationary random variation of the form

$$\mathbf{r}_k + \mathbf{e}_k$$

where $\mathbf{e}_k$ is multivariate (possibly approximately normal) with zero mean and variance/covariance matrix $\mathbf{S}_k$. It is assumed for this paper that a class is spectrally characterized by $\mathbf{r}_k$ and $\mathbf{S}_k$ (for approximate normality), but some spatial information (such as an autocorrelation matrix) could be added without changing the method described here.

If $\mathbf{S}_k$ is approximately the same for each (sub-) class, then the unmodified residual image is the most appropriate display. However, if $\mathbf{S}_k$ varies greatly from class to class, which is always the case for land-cover classes which have not been subdivided into spectral sub-classes, then the residual should be standardized by dividing each channel residual by the square root of the appropriate diagonal element of $\mathbf{S}_k$ in each class. This new standardized (or 'Student's t') image removes variations in the residuals due only to the different signature variance of different types of land cover, by displaying 'standard deviations' from the class mean rather than unmodified residuals.

During the development of the method of residual images, a number of alternative images, such as distance images (grey scale) and absolute value of residual images, were displayed. However, the color coded residual image always provided a more discriminating and useful product.

Mathematically, many of the likelihood based methods of Landsat classification and analysis assume a signature model such as the above. The obvious break-downs of the model, such as class heterogeneity (i.e., unaccounted sub-classes) and non-normality can be assessed through spectral cross plots, histograms, and the residual image itself. The adequacy of the level of precision of the classification can be measured in a variety of ways. In the Example 1 below, tests arising from the analysis of variance between sub-classes (Hope (1968) and the Appendix) are used to assess benefits gained from the retraining and subdivision of classes into spectral sub-classes.

As well as signature (class mean) and class variance and covariance, spatial autocorrelation is a significant source of class specific information in an image (Tubbs and Coberly, 1978). Since the eye can often detect textural and spatial patterns more easily than currently available statistics, the use of the (detrended) residual image to assess this source of information has great potential. However, the methods of texture analysis described in Haralick (1979) can, and should, be applied to the residual image to statistically support such visual analysis.

An example where the stationary signature model breaks down occurs when classes delineate arbitrary sections of an environmental, or spectral, gradient. The within-class trends and patterns are enhanced in the residual image by local contrast stretching, and are quickly picked up by the eye. Since the stationary signature model is not appropriate for such gradients, extended classification methods involving within-class spatial trends for means should be investigated. An example illustrating results which may come from such an extension occurs in Warn (1978), where differences between water depths estimated independently from Bands 4 and 5 are displayed as an image. This image provides an enhancement of turbidity and bottom reflectance as well as an estimate of consistency of the depth map.

Image Display

The relationship between the perceived color differences in both the mean and residual images is related in a complex way to stochastic differences measured in grey levels. Some thought could be given to using a uniform chromaticity scale (MacAdam (1971) or CIE proposal, Anon (1976)) to equate the two.

For this paper a simple linear stretch of the actual grey level range to the full brightness range was applied to the bands displayed. The zero residual was shifted to grey level 63 in each band so that zero and near zero residuals generally appear as mid-grey, and negative residuals are low brightness. However, the color of zero varys with the stretch.

In the light of this, a significant aid to interpreting mean and residual images would be a grey (or color) wedge to scale the differences and indicate the stretched mean values.

Example 1. Land-Cover Mapping

Figure 1 depicts an eight-class land-cover map of a small area (30 km^2) near Batemans Bay on the southeast coast of Australia.

The eight classes were aggregated from a 23-class map used to analyze land-cover separability in the area (Adomeit *et al.*, 1979; Jupp *et al.*, 1979). The 23-class map was produced from 1978, 1:25,000-scale color photography and 1975 black-and-white photography, together with ground data collected in 1979. However, the precise state of the area at the time of the Landsat overpass (October 1975) is not known.

Changes in land cover between the time of the overpass and the acquisition of the aerial photography, as well as uncertainty about the state of the shoals in the bay on 13 October 1975, lead to the following attempt to construct an updated land-cover map from Landsat data using a Bayes classifier. The land-cover map and the October 1975 Landsat Ulladulla scene were registered (as described in Mayo and Jupp (1979)) and a subset of 6640 (83 by 80) pixels from the scene coded to one

FIG. 1. Eight-class land-cover map of Batemans Bay.

TABLE 1. CLASS STATISTICS FOR THE BATEMANS BAY 8 CLASS (ITERATED) LAND-COVER MAP

Class (1) Open water				
Number in class = 1246				
Mean	12.13	8.34	2.87	0.04
Covariance matrix				
	1.58	1.45	.83	0.05
	1.45	2.38	1.14	0.08
	0.83	1.14	1.76	0.09
	0.05	0.08	0.09	0.05
Trace =	5.76			
Class (2) Tidal mudflats and shoals				
Number in class = 305				
Mean	14.12	14.41	11.42	2.77
Covariance matrix				
	7.48	8.78	7.54	2.20
	8.78	12.49	13.23	4.64
	7.54	13.23	32.75	15.56
	2.20	4.64	15.56	8.96
Trace =	61.68			
Class (3) Beaches				
Number in class = 209				
Mean	24.96	31.84	35.05	13.48
Covariance matrix				
	32.90	53.02	61.56	25.56
	53.02	95.56	118.19	53.18
	61.56	118.19	172.82	82.33
	25.56	53.18	82.33	41.27
Trace =	342.55			
Class (4) Wetlands				
Number in class = 723				
Mean	12.44	13.46	22.89	11.28
Covariance matrix				
	2.24	3.00	2.06	0.49
	3.00	6.10	3.91	1.02
	2.06	3.91	10.70	4.62
	0.49	1.02	4.62	3.03
Trace =	22.08			
Class (5) Forests				
Number in class = 2774				
Mean	11.26	11.61	29.94	16.70
Covariance matrix				
	1.03	1.14	1.71	0.87
	1.14	2.55	2.88	1.41
	1.71	2.88	13.54	7.60
	0.87	1.41	7.60	5.36
Trace =	22.48			
Class (6) Suburban and roads				
Number in class = 664				
Mean	16.42	20.20	35.62	17.84
Covariance matrix				
	7.04	11.31	6.27	1.80
	11.31	21.68	10.89	3.12
	6.27	10.89	13.87	5.46
	1.80	3.12	5.46	3.33
Trace =	45.92			
Class (7) Urban				
Number in class = 336				
Mean	22.50	27.19	46.40	22.60
Covariance matrix				
	8.99	11.97	4.05	−0.77
	11.97	20.18	6.40	−1.03
	4.05	6.40	16.62	8.16
	−0.77	−1.03	8.16	6.53
Trace =	52.31			
Class (8) Grassland				
Number in class = 383				
Mean	16.01	17.33	47.25	26.47
Covariance matrix				
	3.94	4.75	9.80	4.42
	4.75	7.88	10.45	4.29
	9.80	10.45	58.78	31.76
	4.42	4.29	31.76	18.91
Trace =	89.51			
Pooled within class covariance matrix				
	3.73	5.15	4.77	1.75
	5.15	9.39	8.17	3.10
	4.77	8.17	19.69	9.78
	1.75	3.10	9.78	6.04
Trace =	38.84			

of the eight classes. The Bayes classifier was trained on the spectral data (Duda and Hart, 1973) for the eight classes, and used to reclassify all of the pixels back into the 'same' eight classes by using maximum likelihood based on means and covariance matrices extracted from a training population from the original eight classes. Twenty-two percent of the pixels were reclassified and the resulting modified map accepted as a final product. As a test, the Bayes classifier was trained on the modified classes, and achieved 95 percent reallocation, but the correction was not reiterated.

Table 1 lists the spectral means and covariance matrices for the reallocated eight classes. As shown by the Trace (sum of diagonal elements, or channel variances), there is considerable difference between class covariance matrices. This difference accounts for the change which occurs when the residual image is standardized. Despite these variations, useful measures of classification precision can be obtained from an analysis of variance into between-class and pooled within-class components. The Appendix describes the measures used here and Table 2 lists them for the two eight-class maps and the 37-class (see below) map. Each measure shows that the increase in class separation due to the above iteration is quite significant.

It can be seen from Plate 1b that the use of spectral data has broadened some of the original classes. For example, highly reflective soils in areas cleared several days before the overpass are grouped with beach sand (I), and some of the dark gullies in the forest classified as wetlands (J). Nevertheless, the mean image represents a clear land-cover map of the area which is readily related to the raw data image (Plate 1a) through the color coding. However, two major differences are apparent:

(1) the color of the Suburban, Roads, and Cleared class is generally disimilar to the corresponding patches in the original image, and
(2) the original image is blurred near boundaries with high contrast, as opposed to the sharpness of the mean image. The possible reasons for (2) above, are:
   (a) atmospheric scattering of light from adjacent pixels into the field of view (Ueno *et al.*, 1978),
   (b) slight band to band misregistration in the raw data, and most importantly
   (c) the removal of mixed pixels at the boundaries of (and on gradients between) classes in the mean image.

Table 2. Measures of Classification Precision for Batemans Bay

Map	Max. λ	$TrW^{-1}B$	X^2	Degrees of freedom
(1) 8 class	6.5	8.5	22271.	28
(2) 8 class iterated	11.5	15.7	30861.	28
(3) 37 class	57.4	71.4	50594.	148

Since the mean image is very sharp, it is apparent that the mean image acts as a low pass filter, but also sharpens edges with strong spectral contrast.

Plates 1c and 1d show, respectively, the residual image and a standardized residual image after the eight land covers have been extracted, and it can be seen that, despite the generally satisfactory agreement between the mean image and the raw data, the eight classes are spectrally quite heterogeneous.

In practice, it is important to keep in mind that similar colors in the residual image do not represent similar land covers, but rather just similar shifts from the class mean. It might be useful in some cases to overlay the class boundaries on the residual image, although it is generally sufficient to be able to view the raw data, and mean and residual images, successively.

Detailed examination of the residual images resulted in the following interpretation of the spectral data:

- There exist strong slope and aspect related variations in irradiance in the northwest forest (D) in both residual images.
- The forest type on the northwest of the image (D) is different from the other forest areas, e.g. (H). Soils, geology, and vegetation changes are known to be associated with this separation (Austin and Cocks, 1978) although it is not easily seen in aerial photographs. Although interpretable in the residual image (Plate 1c) the distinction is most clear from the Band 7 (red) residual in the standardized residual image (Plate 1d). At least three sub-classes of forest (Class 5) are needed to account for these effects.
- There exist strong differences between the golf course (A) and other grassland areas (B, C) in the unstandardized residual). At least two sub-classes are therefore needed for the Grassland class (Class 8).
- In the Suburban Roads and Cleared class (Class 6) there is a need to separate suburban from cleared areas, that is, to map more land-cover classes. This is clear in both residual images.
- There exist several sub-classes of beach. The different sub-classes probably account for variations in brightness due to different slopes and aspect to the sun.
- The estuarine channel (E) is strongly distinguished in the standardized residual image from the submerged sand bar (F) and the shallow open estuarine areas (G).

Using this analysis as a guide for training set selection, the image was further subdivided to 37 (sub-) classes. Table 2 demonstrates the significant increase in discrimination (and therefore preci-

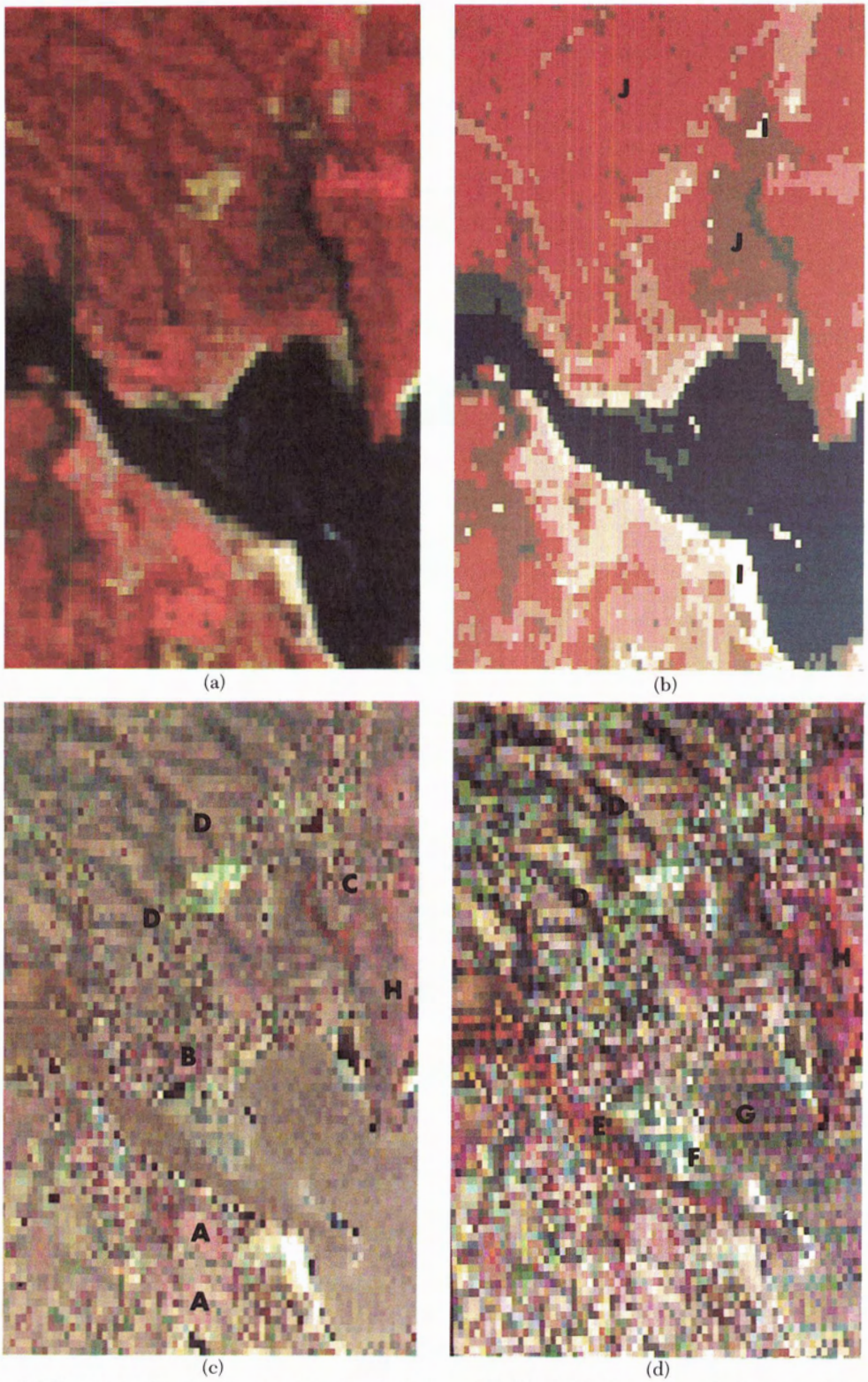

(a) (b) (c) (d)

PLATE 1. (a) Batemans Bay image, raw data Bands 4, 5, and 7. (b) Eight-class map coded to Landsat pixels. (c) Residual image from eight-class map. (d) Standardized residual image.

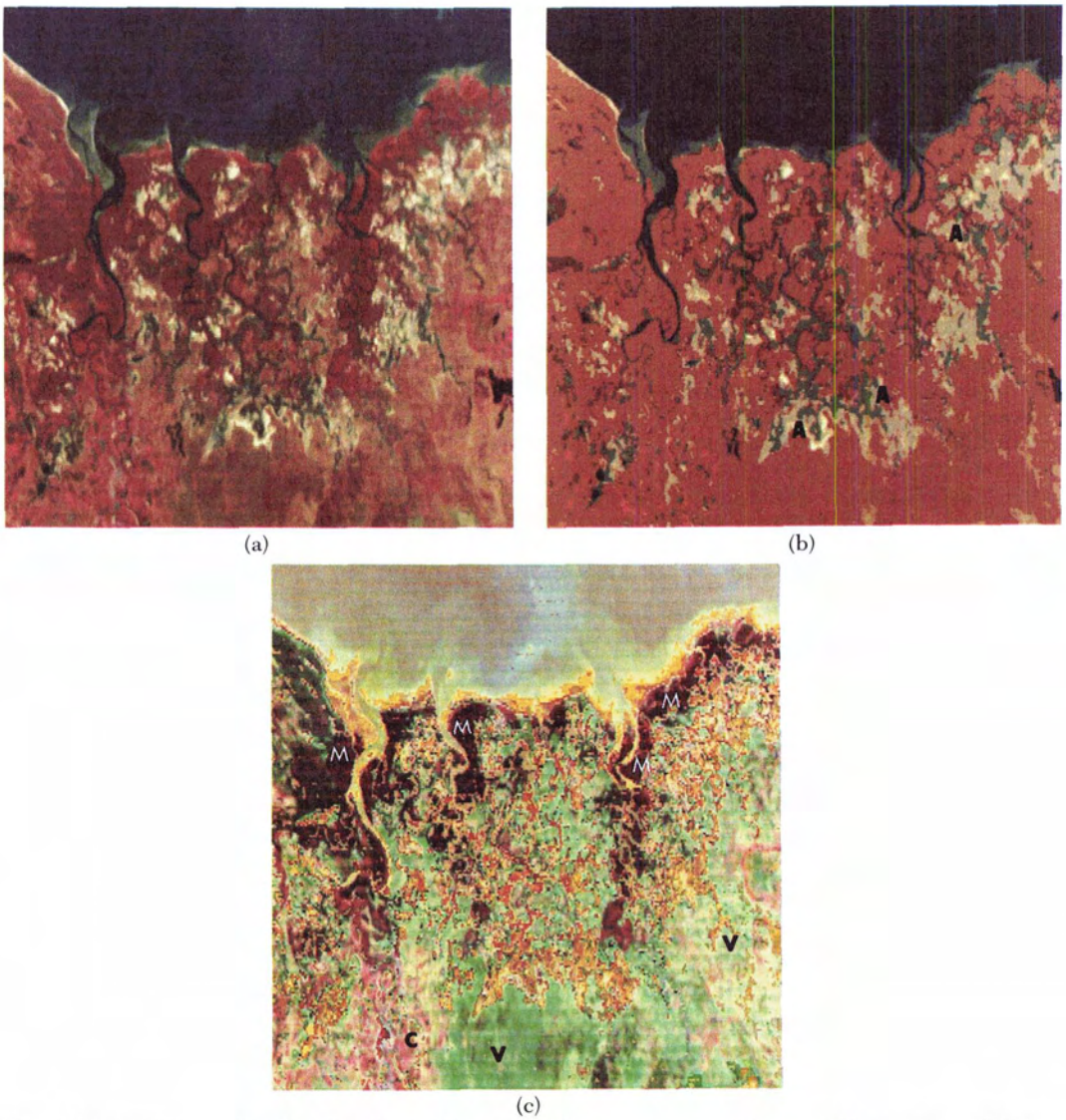

(a) (b)

(c)

PLATE 2. (a) Ayr scene, raw Landsat data Bands 4, 5, and 7. (b) Ayr scene, mean image. (c) Ayr scene, residual image (not standardized).

sion) achieved in this way. The residual image lost much of its structure and the mean image became only marginally different from the raw data. These sub-classes may be grouped into an eight-class system in a way to be reported separately. However, the important point for this paper is that the residual image provided systematic interactive location of new training sites for the 37 sub-class classification.

Briefly, the mean image and residual image together show the major land covers and provide a visual estimate of precision of the land-cover image as measured by Landsat spectral data. In this example, the residual image is dominated by the high variance of the residuals in the beach and cleared and suburban classes and the standardized residual is needed to bring out the more subtle sub-class structure of the other classes.

EXAMPLE 2. SPECTRAL CLASS MAPPING

As a means of spectral class mapping for pattern enhancement, an adaptation of the STANSORT classifier (Honey *et al.*, 1974) has been used together with the mean/residual images. The classifier is a one-pass parallelipiped algorithm, and the 'mean' image is obtained by giving each pixel the mid-value of the defining parallelipiped of its class. This very simple algorithm was chosen since, in this context, the mean and residual images are constructed as image enhancements in 'real time.'

Either the mean or residual image can be displayed as it is computed, and the process halted if the parallelipiped definition seems inadequate.

The method has been applied in two ways. Firstly, the spectral tolerances (or parallelipiped size) can be reduced until the residual is spatially 'random,' and the mean image used as a filtered image. Secondly, the tolerances can be kept very broad, in which case the residual image is the interesting image as an enhancement of background patterns dominated by the spectral differences between major 'classes' in the raw data.

An example of the use of a residual image to enhance subtle patterns in this way has been constructed in a coastal saltmarsh area near Ayr on the northeast coast of Australia. The raw data image is shown in Plate 2a and consists of a subset of 256 lines by 512 pixels from the Ayr scene. For display, the lines are repeated, so that Plate 2a represents a full 512 by 512 screen of data, or approximately 1:80,000 scale.

The mean image (Plate 2b) is the result of using a broad parallelipiped size, and consists of 21 spectral classes. The major classes are associated with the saltmarshes, and especially the margins of bright sand (A). The vegetation beyond the saltmarsh is lumped into a single category at this level, and little of the information in the sea is differentiated. The residual image is shown in Plate 2c, where the mangroves (M), the cane farms (C), and the coastal vegetation (V) clearly separate. The spectral variations in the water near to the coast are also strongly enhanced.

As an analysis of the classification as such, the residual image betrays both the lack of training and the simplicity of the classifier. However, as an enhancement, the residual portrays a number of patterns not easily visible in the raw data which can be located as training sets for a more refined classification method.

Conclusion

The method described consists of developing two images from a classification. These are

- A mean image in which the pixels in the class are assigned the class mean, and
- A residual image in which the pixels are assigned the difference between the raw data and the mean.

The images have a wide variety of uses and offer the possibility of using the standard methods of image analysis to assess the classification. The method can be used to evaluate the precision of a classification, so that inadequate training and overly coarse classification can be refined, or to provide an enhancement of the data which behaves as a non-stationary high-pass filter. The method is recommended as standard practice.

Although applied here to Landsat data, the method is quite general, and may be applied in any spatial data, such as gridded geographical data and digitized photography, which may be analyzed using image display.

Acknowledgments

The authors would like to express their thanks to Drs. D. J. Carpenter and J. F. O'Callaghan for their helpful suggestions and criticisms. Also, the referees improved the original draft of the paper with their constructive criticisms. Dr. P. F. Crapper provided the final version of Figure 1.

References

Abotteen R. A., 1979. Image and numerical display aids for manual interpretation. *The Lacie Symposium, Proceedings of the Technical Sessions, Volume II.*, NASA.

Adomeit, E. M., D. L. B. Jupp, C. Margules, and K. K. Mayo, 1979. The separation of traditionally mapped land cover classes by LANDSAT data, in *Proceedings, Vegetation Classification in Australia Region*, A. N. Gillison and D. J. Anderson (eds), CSIRO/ANU Press), (in press).

Anon, 1976. *Proposal for study of uniform color spaces and color-differences evaluation.* CIE's Compte Rendu 18e Session, Publication CIE N 36, 171 p.

Austin, M. P., and K. D. Cocks, 1978. *Land use on the south coast of New South Wales.* (4 volumes). CSIRO, Australia.

Duda, R. O., and P. E. Hart, 1973. *Pattern Classification and Scene Analysis.* John Wiley and Sons, New York, pp. 405-424.

Haralick, R. M., 1976. Automatic Remote Sensor Image Processing. *Topics in Applied Physics*, Vol. 11, pp. 5-63.

———, 1979. Statistical and structural approaches to texture. *Proceedings of the IEEE*, Vol. 67, No. 5, pp. 786-804.

Honey, F. R., A. Prelat, and R. J. P. Lyons, 1974. STANSORT: Stanford Remote Sensing Laboratory pattern recognition and classification system. *Proceedings 9th International Symposium of Remote Sensing of Environment*, Vol. 2, pp. 897-905. ERIM, Ann Arbor, Michigan.

Hope, K., 1968. *Methods of multivariate analysis.* Univ. of London Press, 288 p.

Joreskog, K. G., 1973. A general method for estimating a linear structural equation system, in *Structural Equation Models in the Social Sciences.* Seminar Press, Inc., New York and London.

Jupp, D. L. B., E. M. Adomeit, M. P. Austin, P. Furlonger, and K. K. Mayo, 1979. The separability of land cover classes on the south coast of N.S.W. *Proceedings, First Australian LANDSAT Conference*, A. A. Green (ed.), (in press).

MacAdam, D. L., 1974. Uniform color scales. *J. Opt. Soc. Am.*, 64, p. 1691.

Mayo, K. K., and D. L. B. Jupp, 1979. Technical problems with raw LANDSAT data. *Proceedings, First*

Australian LANDSAT Conference, A. A. Green (ed.), (in press).

Murai, S., 1975. Evaluation of land use and its color representation in Tokyo district with LANDSAT digitial data. *Proceedings of the 10th International Symposium on Remote Sensing of Environment*, Vol. I, pp. 345-350. Environmental Research Institute of Michigan, Ann Arbor, Michigan.

Roy, S. N., R. Guanadesikan, and J. N. Svivastava, 1971. *Analysis and design of certain quantitative multi response experiments*. Pergamon Press, Oxford.

Tubbs, T. D., and W. A. Coberly, 1978. Spatial correlation and its effect upon classification results in LANDSAT. *Proceedings of the 12th International Symposium on Remote Sensing of Environment*, Vol. II. Environmental Research Institute of Michigan, Ann Arbor, Michigan.

Ueno, S., Y. Haba, Y. Kawata, T. Kusaka, and Y. Terashita, 1978. The atmospheric blurring effect on remotely sensed earth imagery, in *Remote Sensing of the Atmosphere-Inversion Methods and Application*, L. Alain Fymat, E. Venandomeir, and Euev (eds), Elsevier, Amsterdam.

Warne, D. K., 1978. *LANDSAT image analysis: application to hydrographic mapping*. Dept. of Engineering Physics, Technical Report EP-T 22. The Australian National University, Canberra.

Wyszecki, G., and W. S. Stiles, 1967. *Color Science*. John Wiley and Sons, New York.

(Received 30 July 1980; revised and accepted 26 August 1981)

Appendix—Measures of Classification Precision

A1. Analysis of Variance

Let $\mathbf{x}_{ij}$ be the vector of k channel values for the j^{th} of the n_i pixels making up class i out of q classes, and let

$$N = \sum_{i=1}^{q} n_i$$

be the total number of pixels classified.

The total sum of squares and cross products matrix about the grand mean radiance ($\mathbf{x}..$) for all pixels can be decomposed into 'between' and 'within' class covariance matrices as follows:

$$\mathbf{T} = \sum_{i=1}^{q} \sum_{j=1}^{n_i} (\mathbf{x}_{ij} - \bar{\mathbf{x}}..)\,(\mathbf{x}_{ij} - \bar{\mathbf{x}}..)^{\mathrm{T}}$$

$$= \sum_{i=1}^{q} n_i\,(\bar{\mathbf{x}}_{i.} - \bar{\mathbf{x}}..)\,(\bar{\mathbf{x}}_{i.} - \bar{\mathbf{x}}_{..})^{\mathrm{T}}$$

$$+ \sum_{i=1}^{q} \sum_{j=1}^{n_i} (\mathbf{x}_{ij} - \bar{\mathbf{x}}_{i.})\,(\mathbf{x}_{ij} - \bar{\mathbf{x}}_{i.})^{\mathrm{T}}$$

$$= \mathbf{B} + \mathbf{W}$$

This analysis of variance and covariance is algebraically valid whatever assumptions are made about $\mathbf{x}_{ij}$. However, if the $\mathbf{x}_{ij}$ are normally distributed ($N(\boldsymbol{\mu}_i, \boldsymbol{\Sigma})$) with each class having the same covariance matrix, $\boldsymbol{\Sigma}$, then the class mean $\mathbf{x}_{i.}$ and the pooled dispersion matrix

$$\mathbf{V} = \frac{1}{N - q}\,\mathbf{W}$$

are efficient estimates for $\boldsymbol{\mu}_i$ and $\boldsymbol{\Sigma}$, and hypothesis tests may be developed which are useful measures of the separation of the classes.

For this paper, the term 'increased precision' is taken to mean a finer classification in which the classes are still well separated, and although the ideal assumptions for the tests often do not hold, they can be used to make decisions such as when to stop subdividing into sub-classes.

A2. Tests for Separation and Precision

The canonical variates (Hope, 1968) for the analysis are the coefficients ($\boldsymbol{\nu}$) of the linear combinations of the original channels which maximize the ratio of between to within class variance

$$\lambda = \frac{\boldsymbol{\nu}^{\mathrm{T}}\,\mathbf{B}\,\boldsymbol{\nu}}{\boldsymbol{\nu}^{\mathrm{T}}\,\mathbf{W}\,\boldsymbol{\nu}}$$

subject to some constraint, such as $\boldsymbol{\nu}^{\mathrm{T}}\,\mathbf{W}\,\boldsymbol{\nu} = 1$. It may be shown that the canonical variates, and values of the ratio are solutions of the generalized eigen problem

$$\mathbf{B}\boldsymbol{\nu} = \lambda\,\mathbf{W}\,\boldsymbol{\nu}$$

Further, the λ's are also eigenvalues of the product $\mathbf{W}^{-1}\mathbf{B}$, and measure the discriminating power provided by the associated canonical variate.

The three tests based on this analysis are

(i) Wilks Λ (Hope, 1968) $L = \dfrac{|W|}{|T|} = \prod_{i=1}^{k} \left(\dfrac{1}{1 + \lambda_i}\right)$

(ii) Maximum λ

and

(iii) Trace $(\mathbf{W}^{-1}\mathbf{B})$ $\qquad \mathrm{Tr}(\mathbf{W}^{-1}\mathbf{B}) = \sum_{i=1}^{k} \lambda_i.$

Distributional properties for (ii) and (iii) for normally distributed $\mathbf{x}_{ij}$ can be found in Roy *et al.* (1971). For (i), assuming that the $\mathbf{x}_{ij}$ are normally distributed, and that the class covariance matrices are equal, then

$$X^2 = -\left[N - 1 - \tfrac{1}{2}\,(q + k)\right] \log L$$

would be distributed as χ^2 with $k(q-1)$ degrees of freedom. This value is recorded in Table 2, and has been used as follows:

(a) If the number of classes is increased (by splitting classes or adding new training sets), the change is acceptable and truly represents an increase in precision if the increase in χ^2 is significant relative to the increase in degrees of freedom.
(b) If the number of classes is reduced (by removing or aggregating classes) the change is acceptable and represents no loss in precision if the decrease in χ^2 is not significant relative to the decrease in degrees of freedom.

The importance of the work reported in this paper for this process is that increasing the number of (sub-)classes by adding new training sets delineated in the residual image is usually far more satisfactory than computer subdivision of existing spectral classes.

ISPRS Inter-Congress Symposia

Midway between its quadrennial Congresses, each of the technical commissions of the International Society for Photogrammetry and Remote Sensing holds a symposium. Those symposia scheduled for 1982 are listed below.

Commission I*
Advances in the Quality of Image Data
Canberra, Australia
14-16 April 1982

Commission II*
Advances in Instrumentation for Processing and Analysis of Photogrammetric and Remote Sensing Data
Ottawa, Canada
30 August-4 September 1982

Commission III*
Mathematical Models, Accuracy Aspects, and Quality Control
Helsinki, Finland
7-11 June 1982

Commission IV
Computer Assisted Photogrammetry and Cartography
Washington, D.C., U.S.A.
23-27 August 1982

Commission V*
Precision and Speed in Close-Range Photogrammetry
York, England
5-11 September 1982

Commission VI*
Facing the Future of Scientific Communication, Education, and Professional Aspects, Including Research and Development
Mainz, Rathaus, Fed. Rep. of Germany
22-25 September 1982

Commission VII
Operational Utilization and Interpretation of Remote Sensor Data
Toulouse, France
13-18 September 1982

* Calls for papers have been published in *Photogrammetric Engineering and Remote Sensing* for these Commission Symposia as follows:

Commission I, September 1981, page 1372
Commission II, September 1981, page 1342
Commission III, September 1981, page 1325
Commission V, March 1981, page 364
Commission VI, April 1982, page 643
Commission VII, December 1981, page 1754